Fluorescence Correlation Spectroscopy 3. Uniform Translation and Laminar-Flow

ARTICLE *in* BIOPOLYMERS · FEBRUARY 1978

Impact Factor: 2.39 · DOI: 10.1002/bip.1978.360170208

3 AUTHORS, INCLUDING:

Douglas Magde
University of California, San Diego
103 PUBLICATIONS **8,283** CITATIONS
SEE PROFILE

Watt W Webb
Cornell University
418 PUBLICATIONS **42,880** CITATIONS
SEE PROFILE

Fluorescence Correlation Spectroscopy. III. Uniform Translation and Laminar Flow

DOUGLAS MAGDE, *Department of Chemistry, University of California, San Diego, La Jolla, California 92093;* WATT W. WEBB, *Department of Applied Physics, Cornell University, Ithaca, New York 14853;* and ELLIOT L. ELSON, *Department of Chemistry, Cornell University, Ithaca, New York 14853*

Synopsis

We extend fluorescence correlation spectroscopy to systems that undergo translation or laminar flow in a sample cell. We include theoretical and experimental results; we consider uniform and nonuniform velocity profiles. Concentration correlation analysis extracts microscopic rate parameters from measurements of the spontaneous concentration fluctuations, which occur even at equilibrium. Fluorescence is one of the most sensitive means of monitoring these fluctuations. Analysis of flowing or translating systems (1) offers a method of measuring number concentrations of selected species, for example, of aggregates or polymers, (2) provides a nonperturbing velocity probe, (3) sometimes allows one to circumvent photolytic degradation, (4) has proved extremely helpful in testing and aligning apparatus for fluorescence correlation measurements and in verifying theoretical analyses, and (5) may be required for interpretation of results obtained on systems in motion, even though that motion is undesired or initially unsuspected. We include both theoretical and experimental results for combined Poiseuille flow and diffusion in the geometry which is of most practical interest. Theoretical expressions for the much simpler cases of nondiffusive Poiseuille flow as well as uniform flow or translation with or without diffusion constitute limiting cases which are displayed explicitly.

INTRODUCTION

Fluorescence correlation spectroscopy is a new technique for measuring chemical kinetic rates and molecular hydrodynamic parameters by observing the time course of spontaneous concentration fluctuations, which occur even at equilibrium in unperturbed systems.[1-3] Fluorescence is used to monitor, as a function of time, the number of molecules of a particular sort located within a well-defined and very small sample volume. If the molecules are in contact with a reservoir, either because the volume is open or because they are in chemical equilibrium with other reactants, their number will fluctuate. Even though each fluctuation is unpredictable, the mean-square fluctuation amplitude and the characteristic persistence time for fluctuations (more completely, the concentration correlation function) are related to equilibrium and kinetic system parameters. Since the fluctuations vary in time, kinetic parameters become accessible and may be measured even though the system remains always at thermodynamic equilibrium. Theoretical analysis[2] (EM) and experimental examples[3]

Biopolymers, Vol. 17, 361–376 (1978)

0006-3525/78/0017-0361$01.00

(MEW) have been reported for instances involving diffusion and chemical reaction.

In this paper we generalize the formulation FCS to systems undergoing steady, but not necessarily uniform, motion relative to the light beam which defines the sample region. The system contains one or more fluorescent components that may diffuse. For simplicity, however, we exclude chemical reactions. Examples include a liquid solution flowing through a cell past an illuminating beam, a membrane or a sample cell being translated past a probe beam, or a beam scanning a stationary surface or volume. Such configurations could be useful in characterizing aggregation and other properties in macromolecular solutions, in investigating hydrodynamic flow, and in testing or interpreting the parameters of stationary fluorescence correlation spectroscopy experiments. Recently, similar concepts were used to develop a method for measuring the molecular weights of macromolecules.[4] The experimental configuration was, however, different in important details from those we consider.

We begin with the formalism of EM,[2] simply rewriting the necessary equations with an additional term to account for the translational velocity. We outline the solution of the governing differential equation and obtain explicit expressions for the quantity which is of experimental interest, namely, the photocurrent autocorrelation function, for five particular instances: pure diffusion, uniform translation without diffusion, Poiseuille or laminar flow without diffusion, uniform translation with diffusion, and Poiseulle flow with diffusion. The notation is consistent with EM[2] and MEW.[3] We have tried to define briefly all symbols, particularly as they relate to experimental parameters, but we do not repeat all the underlying formalism of EM.[2]

All of the cases considered are experimentally accessible, at least in a limiting sense. But the last leads to the most interesting and novel behavior, as well as the most difficult analysis, so we present experimental data for that instance. We examined the fluorescent dye rhodamine 6G undergoing combined Poiseuille flow and diffusion. Finally, we comment on specific experimental configurations of fluorescence correlation analysis, useful for practical measurements, which lead to the several limiting cases analyzed.

Fluorescence correlation spectroscopy has been extended theoretically to treat also rotational diffusion.[5–8] We ignore that contribution to the correlation function here since it typically occurs on a much shorter time scale than the behavior we do consider. We emphasize also that fluorescence correlation spectroscopy is but one of a number of possible means of implementing concentration correlation analysis, differing in their method of monitoring concentrations. Conductimetric[9] and light-scattering[10,11] techniques have been demonstrated. Two recent reviews[12,13] elaborate on the similarities and differences among these several approaches. We generally prefer the fluorescence method because of its combination of sensitivity with molecular selectivity.

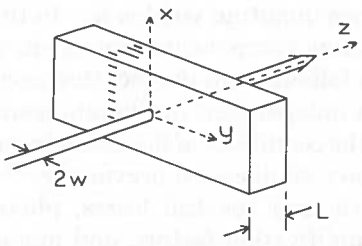

Fig. 1. Schematic arrangement of the experiment: a laser beam incident along $\hat{z}$ passes through a thin sheet of fluorescent solution or membrane which is flowing in the $\hat{y}$ direction. The velocity is uniform over the $\hat{x}\hat{y}$ plane but may vary for different $\hat{z}$.

Photocurrent Correlation Functions

The geometry of the sample region is shown in Fig. 1. The sample is a thin sheet moving in the $\hat{y}$ direction, perpendicular to the excitation laser beam which propagates along $\hat{z}$. The dimensions of the sheet in the $\hat{x}$ and $\hat{y}$ directions are much larger than both the laser beam diameter and the sheet thickness. The velocity of translation or flow in the sheet is constant in time and uniform in the $\hat{x}\hat{y}$ plane over the dimensions of interest. The velocity, however, may vary along $\hat{z}$. We consider two cases explicitly: uniform translation:

$$\mathbf{V}(z) = V\hat{y} \tag{1a}$$

and Poiseuille flow:

$$\mathbf{V}(z) = (4V_m/L^2)z(L - z)\hat{y} \tag{1b}$$

Such a parabolic field is characteristic of the flow of real fluids between parallel plates. In both bases, $\mathbf{V}(z)$ is defined over the region $0 < z < L$, which constitutes the entire length of the illuminated region in view of the fluorescence detector.

The intensity profile of the laser beam defines the cross-sectional area of the sample region. A Gaussian radial intensity distribution is convenient both experimentally and theoretically:

$$I(\mathbf{r}) = I_0 \exp[-2(x^2 + y^2)/w^2] \tag{2}$$

The total laser power is

$$P = \int\int I(\mathbf{r})dxdy = I_0\pi w^2/2 \tag{3}$$

A second possible intensity distribution would be one uniform over a circular disk. Some results for that case were derived previously by EM[2] and an analogous development would be straightforward for the present experiment.

The photocurrent generated in a fluorescence detector is

$$i(t) = g\epsilon Q\int I(\mathbf{r})C(\mathbf{r}, t)d^3\mathbf{r} \tag{4}$$

Here we specialize to the case of a single fluorescent species whose concentration at position $\mathbf{r}$ at time t is $C(\mathbf{r}, t)$, whose molar absorbance is ϵ,

and whose fluorescence quantum yield is Q. In the absence of chemical reaction, several emitting components, if present, would behave entirely independently. This follows from the fact that each fluorescent molecule is to be treated as an independent incoherent source for the fluorescent radiation field under the conditions of fluorescence correlation spectroscopy experiments, as we have emphasized previously.[1-3,12,13] The prefactor g incorporates geometric and spectral losses, photoelectric responsivity factors, electronic amplification factors, and numerical conversion constants. In general, an integral over the fluorescence band is implicit in order to account for varying spectral sensitivity of the detection optics. Optically thin samples are assumed.

The mean, or time-average, photocurrent is

$$\langle i \rangle = gPL\epsilon Q\overline{C} \tag{5}$$

Here, $\overline{C}$ is the ordinary thermodynamic (mean) concentration.

The temporal autocorrelation of the photocurrent is given by Eq. (16) of EM.[2] For a single fluorescent species, it becomes

$$G(\tau) = (g\epsilon Q)^2 \int I(\mathbf{r})I(\mathbf{r}')\phi(\mathbf{r}, \mathbf{r}', \tau)d^3\mathbf{r}, d^3\mathbf{r}' \tag{6}$$

The concentration autocorrelation function ϕ is given by the ensemble average of the concentration fluctuations δC

$$\phi(\mathbf{r},\mathbf{r}',\tau) = \langle \delta C(\mathbf{r},0)\delta C(\mathbf{r}',\tau) \rangle \tag{7}$$

Statistically stationary behavior has been involved in setting the reference time equal to zero.

In Eq. (6) we write only the "interesting" portion of the complete current autocorrelation. We have dropped the *dc* component, which may be experimentally eliminated by analogue electronic filtering in our apparatus, as well as the uncorrelated "shot noise" component, which contributes a spike at $\tau = 0$.

For ideal solutions (normally an excellent approximation in fluorescence correlation spectroscopy), $\phi(\mathbf{r},\mathbf{r}',0) = \overline{C}\delta(\mathbf{r} - \mathbf{r}')$. Hence, we have immediately

$$G(0) = (g\epsilon Q)^2 P^2 L\overline{C}/\pi w^2 \tag{8}$$

The mean concentration $\overline{C}$ refers to the concentration of whatever unit constitutes the mobile independent molecular "particles" whose motion into and out of the volume is to be studied. In particular, if the fluorescent molecules are moving as dimers or higher polymers, $G(0)$ reveals this. The optical parameters ϵ and Q must refer to these "particles."

From Eqs. (5) and (8) we have the result expected for a Poisson distribution, independent of the details of the relaxation processes which determine the complete $G(\tau)$, that the relative mean-square fluctuation is given by

$$G(0)/\langle i \rangle^2 = [\pi w^2 L\overline{C}]^{-1} \tag{9}$$

In order to calculate $G(\tau)$, we first evaluate $\phi(\mathbf{r},\mathbf{r}',\tau)$. According to the

"fluctuation dissipation theorem," ϕ can be interpreted in terms of the dissipation of a small macroscopic perturbation. For dissipation by diffusion and flow, the governing hydrodynamic equation, to be solved with appropriate boundary conditions, is

$$\frac{\partial \delta C(\mathbf{r},\tau)}{\partial \tau} = D\nabla^2 \delta C(\mathbf{r},\tau) - \mathbf{V}(\mathbf{r}) \cdot \nabla \delta C(\mathbf{r},\tau) \tag{10}$$

Here, D is the translational diffusion constant. We have assumed isotropic diffusion, which will obtain in the absence of orientation of anisotropic particles by rapid flow. Equation (10) is discussed in the literature of heat transfer. Unfortunately, it does not separate and is tractable only with restrictive assumptions. We are aware of no previous treatment suitable for our particular geometry, which is unusual in that the boundary conditions are determined by the laser beam rather than physical walls. This permits flow "across" the cylindrical region. We turn, therefore, to specific cases.

Pure Diffusion

When $\mathbf{V}(\mathbf{r}) = 0$, only diffusion is possible. This situation was treated in EM,[2] where Eqs. (22), (21), and (20b) showed, for a single fluorescent species,

$$\phi(\mathbf{r},\mathbf{r}',\tau) = \frac{\overline{C}}{4\pi DL\tau} \exp\left\{-\frac{(x-x')^2 + (y-y')^2}{4D\tau}\right\} \times \left(1 + 2\sum_n \exp\left[-D\left(\frac{n\pi}{L}\right)^2 \tau\right] \cos\frac{n\pi z}{L} \cos\frac{n\pi z'}{L}\right) \tag{11}$$

and

$$G(\tau) = [(g\epsilon Q)^2 P^2 L\overline{C}/\pi w^2][1 + (\tau/\tau_d)]^{-1} \tag{12a}$$

where

$$\tau_d = w^2/4D \tag{12b}$$

Uniform Translation without Diffusion

When $D = 0$, Eq. (1a) may be substituted into Eq. (10) to give

$$\frac{\partial \delta C(\mathbf{r},\tau)}{\partial \tau} = -V \frac{\partial \delta C(\mathbf{r},\tau)}{\partial y} \tag{13}$$

Then, Eq. (7) can be evaluated using the Fourier transform method of EM.[2] However, it follows immediately that

$$\delta C(x,y,z,\tau) = \delta C(x, y - V\tau, z, 0) \tag{14}$$

and ϕ becomes, in terms of the Dirac delta function,

$$\phi(\mathbf{r},\mathbf{r}',\tau) = \overline{C}\delta(x - x', y - y' - V\tau, z - z') \tag{15}$$

Substituting Eq. (15) into Eq. (6) and using Eqs. (2) and (3), we obtain the photocurrent autocorrelation function

$$G(\tau) = \frac{(g\epsilon Q)^2 P^2 L \overline{C}}{\pi w^2} \exp\left[-\left(\frac{V\tau}{w}\right)^2\right] \tag{16}$$

Laminar Flow without Diffusion

For any flow distribution for which the velocity remains oriented along $\hat{y}$ and is a function only of z, the above analysis remains valid with V replaced by $V(z)$.
Then

$$G(\tau) = \frac{(g\epsilon Q)^2 P^2 \overline{C}}{\pi w^2} \int_0^L \exp\left[-\left(\frac{V(z)\tau}{w}\right)^2\right] dz \tag{17}$$

For physically realizable $V(z)$, this integral can always be executed, at least numerically. The situation of most interest is viscous laminar flow between two windows, which leads to the parabolic dependence of Eq. (1b). It is convenient to define

$$\zeta = (2z/L) - 1 \tag{18a}$$

and to introduce the characteristic time

$$\tau_f = w/V_m \tag{18b}$$

Then

$$G(\tau) = [(g\epsilon Q)^2 P^2 L \overline{C}/\pi w^2] F_1(\tau/\tau_f) \tag{19a}$$

with

$$F_1(\tau/\tau_f) = \int_0^1 \exp[-(\tau/\tau_f)^2 (1 - \zeta^2)^2] d\zeta \tag{19b}$$

It is straightforward to develop series expansions for Eq. (19b), which we do in the Appendix. A plot of $F_1(\tau/\tau_f)$ appears in Fig. 2. Note that $F_1(\tau/\tau_f) = G(\tau)/G(0)$.

Uniform Translation with Diffusion

For uniform translation or constant flow velocity throughout the sample volume, as specified by Eq. (1a), the complete Eq. (10) still separates and ϕ may be obtained explicitly:

$$\phi(\mathbf{r},\mathbf{r}',\tau) = \frac{\overline{C}}{4\pi D L \tau} \exp\left\{-\frac{(x - x')^2 + (y - y' - V\tau)^2}{4D\tau}\right\} \times \left\{1 + 2\sum_n \exp\left[-D\left(\frac{n\pi}{L}\right)^2 \tau\right] \cos\frac{n\pi z}{L} \cos\frac{n\pi z'}{L}\right\} \tag{20}$$

This expression may be substituted into Eq. (6), and using Eqs. (2) and (3), we find

$$G(\tau) = \frac{(g\epsilon Q)^2 P^2 L \overline{C}}{\pi w^2 [1 + (\tau/\tau_d)]} \exp\left[-\left(\frac{\tau}{\tau_f}\right)^2 \frac{1}{1 + (\tau/\tau_d)}\right] \tag{21}$$

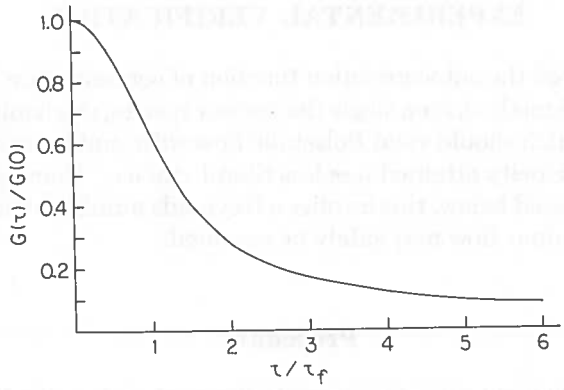

Fig. 2. Photocurrent autocorrelation function for a solution undergoing flow but not diffusion: the parabolic velocity distribution of Poiseuille flow generates a $G(\tau)$ which contrasts with other cases we have calculated in its sigmoidal shape and its very slow decay at long times.

This result is exact and still quite tractable. It reduces to Eq. (16) when $\tau_d \to \infty$, which by Eq. (12b) occurs when the diffusion constant $D \to 0$. When $V \to 0$, we recover Eq. (12). Equation (21) has been derived previously.[14]

Laminar Flow with Diffusion

Once $\mathbf{V}(\mathbf{r})$ is allowed to vary throughout the sample volume as in Eq. (1b), the second term on the right of Eq. (10) couples together motion in orthogonal directions and the differential equation no longer separates. The case which is of most interest in practice has $w \ll L$ (a long, thin, illuminated volume). For this geometry, molecules will diffuse out of the volume before they diffuse very far along it. Then, if the gradient $\partial V(z)/\partial z$ is sufficiently small over most of the region, we can obtain an approximate solution by considering the volume to be made up of a large number of layers perpendicular to $\hat{z}$, in each of which an expression like Eq. (21) holds for the local $V(z)$. These should be integrated to obtain the result

$$G(\tau) = \frac{(g\epsilon Q)^2 P^2 L \overline{C}}{\pi w^2 [1 + (\tau/\tau_d)]} F_2\left(\frac{\tau}{\tau_f}, \frac{\tau}{\tau_d}\right) \tag{22a}$$

with

$$F_2\left(\frac{\tau}{\tau_f}, \frac{\tau}{\tau_d}\right) = \int_0^1 \exp\left\{-\left(\frac{\tau}{\tau_f}\right)^2 \left[1 + \frac{\tau}{\tau_d}\right]^{-1} (1 - \zeta^2)^2\right\} d\zeta \tag{22b}$$

This again may be represented by the same series expansions of the Appendix.

EXPERIMENTAL VERIFICATION

We measured the autocorrelation function of concentration fluctuations, using the FCS method, for a single fluorescent species, rhodamine 6G, under conditions which should yield Poiseuille flow with simultaneous diffusion. The largest velocity attained was less than 1 cm/sec. Combined with the dimensions listed below, this implies a Reynolds number of at most about unity and laminar flow may safely be assumed.

Procedure

The experimental apparatus was similar to that described at length in MEW.[3] Fluorescence was excited by the 514.5-nm line of an argon-ion laser. A continuous power $P = 1$ mW was incident on the sample. The focused beam had a Gaussian profile, as defined in Eq. (2), with parameter $w \approx 4\ \mu$m. The length of the sample volume, $L = 150\ \mu$m along the direction of progogation, $\hat{z}$ in Fig. 1, was set by the windows of a suprasil fused-quartz fluorescence cell. Laminar flow between the cell windows was in the $\hat{y}$ direction. The width of the cell in the $\hat{x}$ direction was $W = 8.0$ mm, which is large, as assumed above.

The fluorescent dye solutions, rhodamine 6G in water, were prepared as reported previously.[3] Data reported here were taken at $\overline{C} = 3.3 \times 10^{-8}$ mol/l. The solution was forced through the sample region with a syringe pump driven by a synchronous motor and variable gear reduction. We verified the absence of leaks to ensure that the volume displaced by the syringe was in fact the volume flowing through the fluorescence cell. Then, we calculated the parameter V_m of Eq. (16) from the volume displacement rate $d\Omega/dt$ and the cell cross-section according to the relation

$$V_m = \frac{3}{2WL}\frac{d\Omega}{dt} \tag{23}$$

The fluorescent emission was detected and the electronic signal processed exactly as previously described.[3] A comprehensive treatment of both statistical and systematic noise was included in that report,[3] relying on unpublished calculations by Koppel. Since then, Koppel[15] has published his rigorous derivation of the random error of concentration correlation measurements. The flow measurements are subject to an additional source of systematic noise not present in previously reported studies. The associated plumbing generated extraneous slow fluctuations which appeared, on the time scale of interest, as a baseline offset. This effect amounted quantitatively to between 2 and 4% of the $G(0)$ of interest. A correction was included in reproducing the data reported below. This improved the curve fitting at long τ, but has a negligible effect on the characteristic times τ_f and τ_d deduced from the entire record.

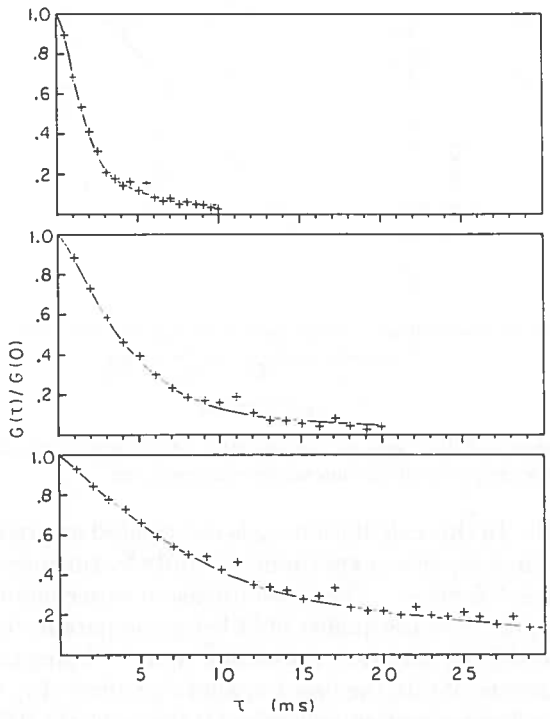

Fig. 3. Experimentally determined autocorrelation functions: the data points and theoretical curves are displayed for a system undergoing simultaneous diffusion and Poiseuille flow. Top: τ_f = 1.4 msec. Center: τ_f = 3.5 msec. Bottom: τ_f = 11 msec. In all cases, τ_d = 11 msec. The original data, accumulated on different times bases for optimum precision, have been redrawn on the same time base in order to show the dramatic change as the pump speed is varied while all other parameters remain fixed. The ordinate was separately normalized for the three cases. The mean $G(0)/\langle i^2 \rangle$ was 7×10^{-6}. Slight modulation of the laser by the active stabilization circuitry is visible.

Results

With the apparatus just described, $G(\tau)$ could be measured over a range of flow velocities varying by a factor of 300 or the flow could be stopped entirely. The three experimental measurements reproduced in Fig. 3 are selected to illustrate and verify Eq. (22) under conditions in which there should be obvious and dramatic dependence of $G(\tau)$ on the flow velocity and yet the effect of diffusion should also be prominent in the record. The three measurements were carried out in succession with nothing changed except the gearing of the syringe pump. This was altered to reduce the flow rate in the ratio 15:6:2. A corresponding increase in the persistence time of concentration fluctuations in the observation volume is qualitatively apparent. At the same time, closer examination reveals that $G(\tau)$ does not simply scale in exactly that ratio. Diffusive processes become increasingly important as the flow rate slows and have a prominent effect, particularly in Fig. 3(bottom). The theoretical curves are calculated using Eqs. (22),

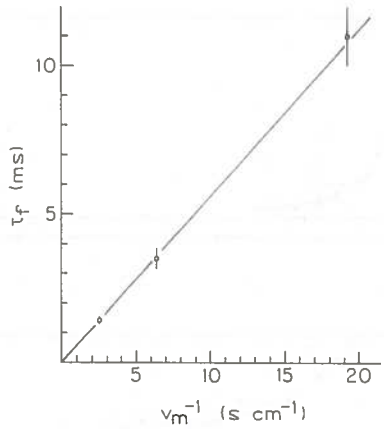

Fig. 4. Dependence of flow time on flow velocity: the characteristic time τ_f is directly proportional to the reciprocal of the flow velocity, as predicted.

(A8), and (A9). In this calculation, τ_d is *not* treated as a free variable. It was measured in a separate experiment (simply by turning off the pump) to be $\tau_d = 11 \pm 0.5$ msec. This pure diffusion experiment was well described by Eq. (12), with the quality of fit being comparable to that reported previously[3] for slightly different values of $\overline{C}$ and w. Using this value of τ_d, the curves drawn to obtain the best fit generate values of $\tau_f = 1.4$, 3.5, and 11 msec for the decreasing flow velocities (a) through (c). The uncertainty of τ_f is not more than about 10%. Since by Eq. (23) V_m is proportional to flow rate $d\Omega/dt$, while by Eq. (18b) τ_f is inversely proportional to V_m, we expect these measured τ_f to vary inversely with the pump speed. This is shown to be the case in Fig. 4. The quantity V_m is known to very high relative precision and even the absolute values, calculated by Eq. (23), should be accurate to well within 10%. From the slope in Fig. 4, using Eq. (18b), we can derive a value for the beam "radius" $w = 5.6 \pm 0.7$ μm. This may be compared with the results of other independent methods of estimating w. These include direct computation from the focusing optics, evaluation from τ_d using Eq. (12b) with the value of D reported previously,[3] and from the amplitude $G(0)$ using Eq. (8) with the value of $\overline{C}$ determined by gravimetric and photometric means. These three were each subject to uncertainties which are somewhat more difficult to evaluate, but must be near ±20%. All three concur in an estimate some 30% smaller than the above, or 4 ± 1 μm. (Note that the characteristic times τ_f and τ_d are obtained directly from curve fitting. Uncertainty in w affects only the derivation of D from τ_f.) There is, therefore, overall agreement among all the independent experimental measurements, within their combined uncertainties. There has also been presented to us a challenge to reduce those uncertainties to the few percent level. Toward that end, the entire instrumentation has been reanalyzed and largely redesigned.[16] Provision has been made to measure w much more simply and accurately by scanning the laser beam past a knife edge. In suitable cases, diffusion measurements

have proven to be reproducible over long periods of time to about ±10%.[17]

APPLICATIONS AND DISCUSSION

We have shown that the extension of fluorescent correlation spectroscopy to systems undergoing steady transport is relatively simple both in theory and in practice. Although we have emphasized flow of a solution of fluorophores through a sample cell, there are other ways of carrying out experiments of this type. For example, the sample cell may be translated past the excitation light beam or the beam may be scanned across the cell. The $G(\tau)$ expected for these types of experiments are presented in Eqs. (16) and (21).

There are several areas in which the correlation analysis of flowing or translating systems may find application. The most immediately useful of its potential is in the measurement of the size or degree of polymerization of fluorescent-labeled particles. Both the initial amplitude and characteristic diffusion times may be useful for this purpose. The initial amplitude, $G(0)$, measures the mean number of independent fluorescent units in solution. Combined with an independent measure of the total solute mass in solution, such a number determination yields molecular weight information.[4] Consider for definiteness the aggregation reaction

$$nA \rightarrow B$$

Then,

$$G(0) = \frac{(gP)^2}{\pi w^2}\left[\overline{C}_A(\epsilon_A Q_A)^2 + \overline{C}_B(\epsilon_B Q_B)^2\right]$$

where B refers to the aggregate oligomer A_n. We suppose that the fluorescence quantum yield and absorption coefficient of the monomer are unaffected by the polymerization reaction: $Q_A = Q_B$; but $\epsilon_B = n\epsilon_A$. Let the fractional progress of the reaction be $\alpha = n\overline{C}_B/\overline{C}_0$, where $\overline{C}_0 = \overline{C}_A + n\overline{C}_B$ is the total A concentration. Then,

$$G(0) = G_0[1 + (n - 1)\alpha]$$

where $G_0 = [(gP)^2/\pi w^2]\overline{C}_0(\epsilon_A Q_A)^2$, the initial amplitude in the presence of the monomer only. Therefore, $G(0)$, which depends linearly on n, provides a sensitive indicator of polymerization and aggregation reactions. For example, if $n = 100$, the polymerization of only 1% of the monomer units ($\alpha = 0.01$) would double $G(0)$. This sensitivity coupled with the wavelength selectivity of fluorescence excitation and emission suggests that fluorometric correlation spectroscopy could provide a useful method for monitoring aggregation reactions in heterogeneous systems such as cytoplasm or serum.

The characteristic times τ_d will also monitor the extent of a polymerization reaction. Since D varies typically as $n^{-1/2}$ to $n^{-1/3}$ in solution, the

temporal behavior of $G(\tau)$ is likely to be a less sensitive indicator than $G(0)$ combined with a concentration measurement.

The extraction of diffusion times obviously requires analysis of the complete $G(\tau)$ and the separation of diffusive components from flow whether the latter occurs by design or accident. In contrast, one might in principle measure $G(0)$ simply as the mean-square photomultiplier noise voltage or current using an ac voltmeter without benefit of full correlation analysis. In practice, however, this measurement almost invariably includes large spurious contributions. Shot noise typically far exceeds the desired $G(0)$ in fluorescence correlation experiments. Hence, $G(0)$ is found by extrapolating $G(\tau)$ back to $\tau = 0$. Shot noise contributes only to the zero delay channel and so is not included in the extrapolation. Countering systematic noise in the record requires not only a simple extrapolation but a detailed curve fitting, for only the fluctuations due to motion of the unit particles into and out of the volume should be included in $G(0)$. It becomes essential, then, that the time scale for molecular motion be set by the experiment in a regime removed from extraneous noise fluctuations. In particular, motion must be fast enough.

For rapidly diffusing particles it is both sufficient and convenient to measure $G(\tau)$ due to simple diffusion in a stationary system. The detection of fluorophore aggregates by fluorescence correlation in this way has already been reported briefly.[16] For systems with slowly diffusing components, however, measurements of the entire $G(\tau)$ for diffusion is difficult and tedious. This is because these experiments require longer integration times to obtain $G(\tau)$ and become more vulnerable to system instabilities. Using a flow or scan technique, one can adjust the velocity to obtain a desired value for τ_f and, thereby, a convenient integration time for $G(\tau)$.

Whether to use a flow or scan method depends on the properties of the system to be analyzed. We have found that the former generates significantly lower levels of systematic interference (unpublished results). Flow systems should be superior for moderate aggregation or for medium-sized molecules with several to a few dozen fluorescent labels. Such experiments require the full analysis presented here.

In the extreme polymer limit, with scores of tags per macromolecule, fluorescence changes due to particle-number fluctuations become very large and dominate the extra noise which results when the excitation beam traverses inhomogeneities in the cell windows. Translation schemes then become practical. In the same circumstances, diffusion will usually be negligible and the simplest analysis, Eq. (16), will suffice. Weissman and coworkers[4] have demonstrated impressive precision in determining DNA molecular weights in this way. To obtain that precision, however, still required an ingenious experimental design and considerable care in the details of construction.

It seems, therefore, that three approaches are emerging by which to exploit fluorescence correlation for number-concentration measurements, each most effective in a particular realm. Other applications of flow studies merit mention but do not require as detailed discussion.

The methods described can, of course, be used to measure flow rates $d\Omega/dt$ or transport times τ_f for dilute fluorescent solutions. As a particular advantage, fluorescence correlation spectroscopy can measure flow in very small systems, such as capillaries or cells. Such flow rates are of interest themselves in biophysical studies. They also provide access to additional molecular parameters.

A combination of a measurement of τ_f in Poiseuille flow, and thus of V_m with a measurement of the pressure gradient α required to drive the flow, for instance, yields a value of shear viscosity $\mu = L^2\alpha/8V_m = L^2\alpha\tau_f/8w$. This result can be combined with a measurement of the diffusion time $\tau_D = w^2/4D$ to obtain the Stokes radius of the fluorescence-labeled molecule $R = k_BT/6\pi\mu D = (k_BT/6\pi)(wL^2\alpha\tau_f/32\tau_d)$. Here, k_BT is the Boltzmann constant times the temperature. The value of R, incidentally, provides yet another measure of the number of monomers n in a polymer or micelle.

Fluorescence as an indicator of molecular motion in number fluctuation experiments can be replaced by scattering, provided the scattering is large. Johnson and Webb employed scattering in a concentration-correlation flow experiment in the turbulent regime. They analyzed number fluctuations associated with the alignment of elongated particles (tobacco mosaic virus) by turbulent eddies.[18,19]

The use of flow or translation techniques can also provide useful support for stationary studies of diffusion or chemical kinetics. It is helpful to test theory and practice using a flow experiment because the characteristic flow time is more easily controlled (by changing the velocity) than are characteristic times for diffusion and chemical kinetics. Indeed, measurements of this kind played an essential role in the development of instrumental techniques for our original studies.[1,3]

Flow or translation also provides a way of avoiding problems due to photolytic destruction of fluorophores by the intense laser excitation beam ($\sim$1 kw/cm^{-2}). In our previous experiments[3] we relied on diffusion to replenish photolyzed fluorophores in the observation region. Since the characteristic diffusion time varies as w^2, a wide range of replenishing times are available. Nevertheless, using a flow system can ensure that even very slowly diffusing components are refreshed at adequate rates and offers more flexibility in the choice of the dimensions of the observation volume.

Finally, the fact that adventitious relative motion between the excitation beam and the solution or the sample cell generates flow or translation components in $G(\tau)$ requires the experimenter to be aware of their form as he undertakes curve fitting, even if no flow is deliberately introduced.

SUMMARY

We have discussed the application of fluorescence correlation spectroscopy to systems in which translational motion and diffusion, but no chemical reaction, occur. We calculated explicit correlation functions,

assuming a Gaussian excitation beam perpendicular to the flow velocity. We find $G(\tau)$ in closed form for uniform translation without diffusion and for uniform translation with diffusion. We find series expansions of an exact integral for Poseuille (laminar, parabolic) flow without diffusion. For the general case of Poiseuille flow with diffusion, we find an approximate expression valid when the cross section of the sample volume is small compared to dimensions over which the flow velocity changes.

We presented experimental data for the combined diffusion and Poiseuille flow of rhodamine 6G in water and demonstrated satisfactory agreement with the theoretical expression.

We concluded with comments on the application of translation and flow in fluorescence correlation studies.

The authors thank Dr. H. Silver for suggesting the Mellin transform. The work was supported in part by the National Science Foundation and the National Institutes of Health. The experiments depended on facilities of the Materials Science Center at Cornell.

APPENDIX

We need to evaluate the integral

$$F(a) = \int_0^1 \exp[-a^2(1-\zeta^2)^2]d\zeta \tag{A1}$$

where a is defined by comparison with Eqs. (19b) and (22b). Power series expansions are readily generated by invoking a Mellin transform:

$$M\{F(a), s\} = \int_0^\infty F(a)a^{s-1}da \tag{A2}$$

After inserting $F(a)$, changing the order of integration, and computing the integral over a, we obtain, in terms of the usual gamma function,

$$M\{F(a), s\} = \tfrac{1}{2}\Gamma(s/2) \int_0^1 (1-\zeta^2)^{-s}d\zeta \tag{A3}$$

which is finite if $\mathrm{Re}(s) > 0$. By defining $t = \zeta^2$, we may write Eq. (A3) in a form recognizable as the integral definition of the usual beta function. Expressing the latter in terms of gamma functions, and collecting factors dependent on s, we have

$$M\{F(a), s\} = \tfrac{1}{4}\Gamma(\tfrac{1}{2}) \frac{\Gamma(s/2)\Gamma(1-s)}{\Gamma[(3/2)-s]} \tag{A4}$$

where now $0 < \mathrm{Re}\,(s) < 1$.

Now we invoke the inverse Mellin transform:

$$F(a) = (2\pi i)^{-1} \int_{c-i\infty}^{c+i\infty} M\{F(a), s\}a^{-s}da \tag{A5}$$

where $0 < c < 1$. We evaluate Eq. (A5) by closing the contour with a large

semicircle, whose contribution to $F(a)$ is zero, and using the Cauchy residue theorem. Considering the functions of s in Eq. (A4), we observe that

$$\text{Res}\left[\Gamma\left(\frac{s}{2}\right)\right] = \frac{2(-1)^n}{n!} \qquad s = -2n \tag{A6a}$$

$$\text{Res}\left[\Gamma(1-s)\right] = \frac{(-1)^{n+1}}{n!} \qquad s = 1+n \tag{A6b}$$

where $n = 0, 1, 2, \ldots$.

An expansion useful for small a is obtained by closing the contour counterclockwise to include the negative real axis. In this case, we use Eq. (A6a) in evaluating Eq. (A5),

$$F(a) = \tfrac{1}{4}\Gamma(\tfrac{1}{2}) \sum_n \text{Res}\left[\frac{\Gamma(s/2)\Gamma(1-s)}{\Gamma(3/2-s)}\right] a^{-s} \qquad s = -2n \tag{A7}$$

to obtain finally

$$F(a) = \tfrac{1}{2}\pi^{1/2} \sum_{n=0}^{\infty} \frac{(-1)^n(2n)!}{n!\Gamma(3/2+2n)} a^{2n} \tag{A8}$$

Although useful for small a, this eventually converges for all a and is, in fact, what would be obtained by expanding the exponential in Eq. (A1) and simply integrating term by term.

An asymptotic expansion more useful for large a is obtained by closing the contour clockwise. Now we use Eq. (A6b) and obtain after some manipulation

$$F(a) = \frac{1}{4a\pi^{1/2}} \sum_{n=0}^{\infty} \frac{\Gamma[(1+n)/2]\Gamma(n+\tfrac{1}{2})}{n!} a^{-n} \tag{A9}$$

References

1. Magde, D., Elson, E. & Webb, W. W. (1972) *Phys. Rev. Lett.* **29,** 705–708.
2. Elson, E. L. & Magde, D. (1974) *Biopolymers* **13,** 1–27.
3. Magde, D., Elson, E. L. & Webb, W. W. (1974) *Biopolymers* **13,** 29–61.
4. Weissman, M., Schindler, H. & Feher, G. (1976) *Proc. Natl. Acad. Sci. USA* **73,** 2776–2780.
5. Ehrenberg, M. & Rigler, R. (1974) *Chem. Phys.* **4,** 390–401.
6. Aragón, S. R. & Pecora, R. (1975) *Biopolymers* **14,** 119–137.
7. Aragón, S. R. & Pecora, R. (1976) *J. Chem. Phys.* **64,** 1791–1803.
8. Yardley, J. T. & Specht, L.T. (1976) *Chem. Phys. Lett.* **37,** 543–546.
9. Feher, G. & Weissman, M. (1973) *Proc. Natl. Acad. Sci. USA,* 870–875.
10. Schaefer, D. W. (1973) *Science* **180,** 1293–1295.
11. Voss, R. F. & Clarke, J. (1976) *J. Phys. A: Math. Nucl. Gen.* **9,** 561–571.
12. Elson, E. L. & Webb, W. W. (1975) *Ann. Rev. Biophys. Bioeng.* **4,** 311–334.
13. Magde, D. (1977) in *Chemical Relaxation in Molecular Biology,* Pecht, I. & Rigler, R., Eds., Springer-Verlag, Berlin, pp. 43–81.
14. Berne, B. J. & Pecora, R. (1976) *Dynamic Light Scattering with Applications to Chemistry, Biology, and Physics,* Wiley-Interscience, New York, p. 107.
15. Koppel, D. E. (1974) *Phys. Rev.* **A10,** 1938–1945.
16. Koppel, D. E., Axelrod, D., Schlessinger, J., Elson, E. L. & Webb, W. W. (1976) *Biophys. J.* **16,** 1315–1329.

17. Fahey, P. F., Koppel, D. E., Barak, L. S., Wolf, D. E., Elson, E. L. & Webb, W. W. (1977) *Science* **195,** 305–306.
18. Johnson, D. H. & Webb, W. W. (1972) *Bull. Am. Phys. Soc.* **17,** 1084.
19. D. H. Johnson, (1974) Ph.D. dissertation, Cornell University.

Received March 14, 1977
Accepted May 19, 1977